Proceedings of the 9th U.S. National and 10th Canadian Conference on Earthquake Engineering
Compte Rendu de la 9ième Conférence Nationale Américaine et
10ième Conférence Canadienne de Génie Parasismique
July 25-29, 2010, Toronto, Ontario, Canada • Paper No 581

THREE DIMENSIONAL MODELING OF TRIPLE FRICTION PENDULUM ISOLATORS

Tracy C. Becker[1] and Stephen A. Mahin[2]

ABSTRACT

This paper presents techniques for modeling triple pendulum isolation bearings subjected to three-dimensional (3-D) excitation. The behavior of the triple pendulum bearing has been described in the XY plane. The XY plane includes the vertical degree freedom and one lateral degree of freedom. However, the bearing behavior is considerably more complex in three dimensions due to the interaction of the four sliding surfaces and their respective restraints. Although shake table tests have shown the bearings to have good performance under three-component earthquake excitations, it is important develop a robust analytical model capable of explicitly capturing the 3-D behavior of each internal component. A non-linear, kinematic model is used in the analysis of the bearing three-component motion. Experiments were conducted using the shake table at the University of California, Berkeley as part of an effort to characterize the 3-D behavior. A comparison between the experimental data and the corresponding results of the kinematic model shows favorable agreement.

Introduction

A triple friction pendulum (TFP) bearing consists of four sliding surfaces acting in series. The inner two surfaces are identical, resulting in three distinct pendulum mechanisms. As the bearing displacement increases, the surfaces on which sliding occurs change, resulting in incremental softening of behavior. As the bearing approaches its ultimate capacity, the displacement restraints of the sliders are reached and the bearing again changes the surfaces on which it slides. This causes incremental hardening behavior until the bearing reaches its ultimate displacement capacity. Because of this behavior, TFP bearings are ideal for performance-based design (Morgan and Mahin 2008). However, there are still some challenges in modeling in the bearing behavior.

Although the 2D (vertical degree freedom and one lateral degree of freedom) behavior of the TFP bearing has been documented (Fenz and Constantinou 2008(a), Morgan and Mahin 2008), the interaction between the four internal slider interfaces makes the 3D behavior far more

[1]Ph.D. Candidate, Dept. of Civil and Environmental Engineering, University of California Berkeley, Berkeley, CA 94720
[2]Professor, Dept. of Civil and Environmental Engineering, University of California Berkeley, Berkeley, CA 94720

complicated. The 2D model is developed by taking the equilibrium at each stage of motion in order to find the force-deformation relationship for that stage. This results in piece-wise linear behavior that requires numerous rules for loading and unloading, which make modeling with this approach very difficult. As a result, models utilizing a series of gap-hook and spring elements were developed to match the 2D piece-wise behavior of the bearing (Fenz and Constantinou 2008(b), Morgan 2007). The spring model cannot track the slider displacements accurately. Current 3D models implement the series model in both X and Y directions. They do not exhibit circular yield surfaces or slider-restraint surfaces. No analytical models previously exist that can track individual slider displacements or slider-restrainer interactions in 3D.

In order to accommodate any 3D motion pattern it is necessary to develop a general bearing model. To do this, a kinematic model based on the constitutive and compatibility relationships of the bearing sliding surfaces is used. Due to the non-linearity of the bearing behavior, these relationships are updated at each displacement increment. Coupled plasticity with a circular yield surfaces as well as circular restrainer surfaces are also necessary to properly describe the bearing motion. Comparison with experimental test data is necessary for the validation of the model.

Kinematic Model

The bearing kinematic model is dependent on both individual slider behaviors and the geometric relationships of the bearing parts. At each displacement increment, the tangent stiffness of the sliding surfaces is calculated, and the transformation matrix from local slider displacements to the global X and Y displacements is updated. The local tangent stiffness and transformation matrices are then used to find the global tangent stiffness matrix. The change in force in the X and Y directions is then found by multiplying the global tangent stiffness vector by the displacement increment.

The vertical deformation of the bearing is calculated from the displacements of the bearing sliders based on their geometry. The internal components of the bearing are each modeled as axially rigid; hence the elastic vertical stiffness is ignored.

Bearing Geometry

Of the four sliding surfaces of the TFP bearing, three can be distinct. Currently implemented TFP bearings have identical geometry for top and bottom inner surfaces. Each distinct sliding surface of the TFP bearing has its own friction coefficient μ, radius R and inner and outer diameter, ID and OD. The effective pendulum length, L, for each surface is taken as $L=R-h$. Where h is the distance from the sliding surface to the center of the bearing. A cross-sectional diagram of a TFP bearing with its geometry is shown in Fig. 1.

Sliding Surface Constitutive Relationship

Each sliding surface has the same general behavior shown in Fig 2., varying only in its yield force, post yield stiffness and displacement limit. Theoretically, motion on a friction surface initiates at an infinitesimally small displacement. However, an infinite stiffness presents

a problem in matrix operations, so the deformation displacement of 0.01in at yield is typically used (Sheller and Constantinou 1999). The initial stiffness, μ divided by 0.01in, is referred to as k_0. The yield force of the slider is dependent on its friction coefficient and the normal force on the slider. The normalized yield force, the yield force divided by the normal load, is simply the slider friction coefficient. After yield, the slider travels with a stiffness inversely proportional to its effective pendulum length. This motion continues until the slider reaches its restrainer displacement. The stiffness after the restrainer displacement is reached is theoretically infinite. To model this, k_0 is again used for the contact stiffness to ensure numerical stability.

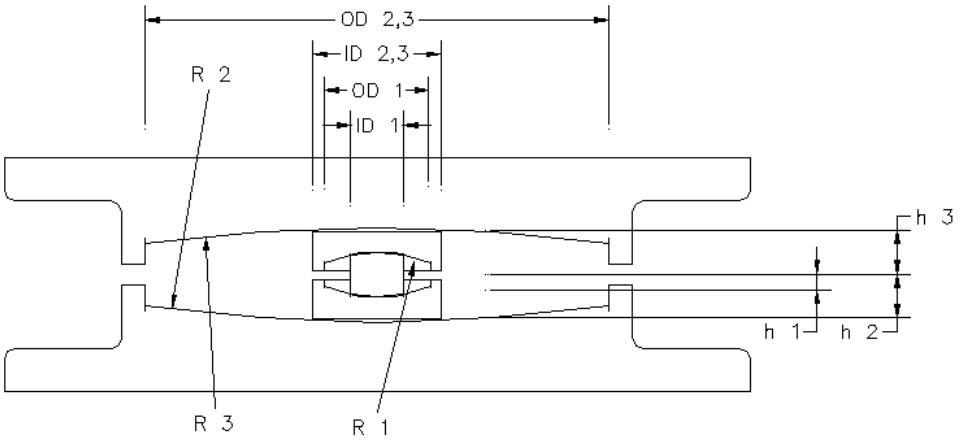

Figure 1. Geometry of TFP bearings.

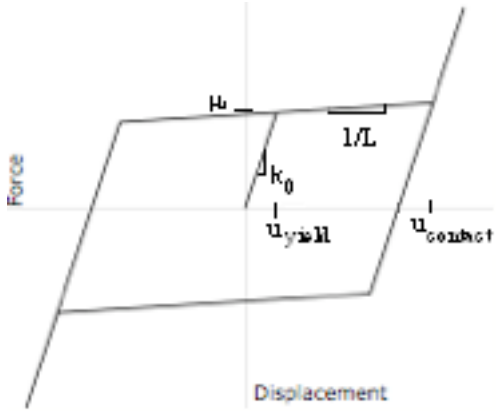

Figure 2. Individual slider behavior.

Bi-Bidirectional Effects

The force-deformation behavior of the sliders is best broken up into three parts: the friction hystereses, the elastic force due to the bearing radius and the contact force. The elastic force contributes a stiffness of $1/L$ at all displacements. The stiffness from the contact force is conditionally applied only when the restrainer is reached. The hysteretic friction force is applied in the direction of instantaneous velocity of the slider. At each displacement increment the direction of the friction force must be updated. This is described by a bi-directional plasticity model and implemented using a return-mapping algorithm (Simo and Hughes 2000). The

methods described by Mosqueda et al. (2004) for modeling the bi-directional plasticity of a single friction pendulum bearing are implemented for each sliding surface of the TFP bearing.

The benefits of using Cartesian coordinates when mapping slider displacements is the ability to use a previously defined return-mapping algorithm to describe the plasticity of the bearing. However, this choice complicates the computation of stiffness due to the slider radius. At each displacement step *i* the effective radius of the slider in both the *X* and *Y* direction must be recalculated using the following equations

$$L_{Xi} = \sqrt{{L_{X0}}^2 - {u_{Yi}}^2} \tag{1a}$$

$$L_{Yi} = \sqrt{{L_{Y0}}^2 - {u_{Xi}}^2} \tag{1b}$$

Where u_X and u_Y are the local slider displacements.

Restrainer Contact

The restrainer surface of each slider has a great effect on the bearing behavior. In order to allow the slider to travel tangentially to the restrainer surface, *X* and *Y* displacements are checked separately for the contact condition. Similarly to the effective radius, the slider restrainer surface must be updated with each new set of local *X* and *Y* displacements. The restrainer distances, u_{RY} and u_{RX}, are found from the equations

$$u_{RXi} = \sqrt{\left(\frac{(OD-ID)}{2}\right)^2 - {u_{Yi}}^2} \tag{2a}$$

$$u_{RYi} = \sqrt{\left(\frac{(OD-ID)}{2}\right)^2 - {u_{Xi}}^2} \tag{2b}$$

If u_X or u_Y exceeds u_{RY} or u_{RX}, respectively, the bearing has contacted the restrainer and the stiffness of the slider in that direction becomes the same as the initial slider stiffness k_0.

Geometric Compatibility Relationship

This model assumes there are rigid floor slabs that resist bending both above and below the isolation level. This assumption restricts the global rotational degrees of freedom of the bearing to zero. The remaining global degrees of freedom are translation in the *X* and *Y* direction. From geometry and the assumption that the top and bottom of the bearing remains parallel it can be found that the displacement in the *X* and *Y* directions of the bearing are equal to the summation of the local displacements on each slider *j*.

$$U_{Xi} = \sum_{j=1}^{4} u_{Xji} \tag{3a}$$

$$U_{Yi} = \sum_{j=1}^{4} u_{Yji} \tag{3b}$$

The local slider rotations θ, shown in Fig. 3, are defined as the angle made from the radii that extend from two bearings pieces that share the same sliding interfaces Furthermore, from the zero rotation assumption, the sum of the local slider rotations θ in the X and Y directions both sum to zero.

$$\sum_{j=1}^{4} \theta_{Xji} = \sum_{j=1}^{4} \theta_{Yji} = 0 \tag{4}$$

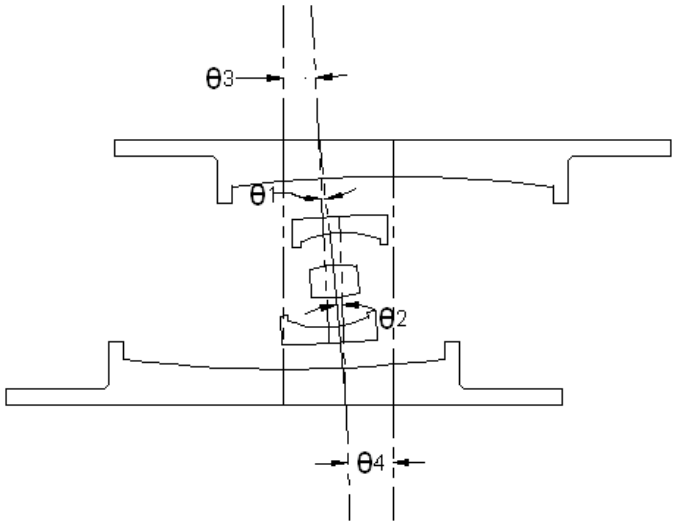

Figure 3. Local slider rotations with the assumption that the outer surfaces of the bearing remain parallel.

The local rotations are directly related to the local displacements by the effective radii.

$$u_i = L_i \theta_i \tag{5}$$

Equations 3, 4, and 5 are used to develop a transformation matrix between the local displacements and the global displacements.

Comparison with Experimental Data

Rigid Block Tests

Characterization tests were run in order to further understand the three-dimensional behavior of the triple friction pendulum bearing. The test set-up, modeled after similar tests done for single friction pendulum bearings (Mosqueda et al. 20004), is shown in Fig. 4. A 68 kip rigid block mass was supported by four TFP bearings on the UC Berkeley shake table. The rigid block consisted of a frame loaded with four concrete bocks. The rigid block was braced with HSS

struts to four reaction blocks rigidly connected off of the shake table platform. The struts kept the frame stationary while the table was moved below, resulting in bi-directional displacement-controlled testing. The displacement-controlled motions included sine waves, circles, squares and figure eights. To investigate the behavior of multiple sliding surfaces, the signals were run with incrementally increasing amplitudes from 0.2 in to 5.0 in. The orbits of these tests can be seen in Fig. 5. All orbit tests were conducted at a velocity of approximately 6in/s. A five-component load cell was located under each bearing to measure and record axial, shear and moment response.

The geometry and friction coefficients of the TFP bearings used in this study are given in Table 1. These bearings, typical of TFP bearings in use, had the same geometry for the outer two sliding surfaces. The effective radii of the inner sliders and outer sliders were 2.5 in and 38 in respectively. The displacement capacity of the bearings was ± 8.2 in. The friction coefficients of TFP bearings cannot be determined without experimental testing. They are determined from a series of force deformation loops at increasing displacement increments.

The force-deformation curves from both the experimental data and the analytical model for the *X* and *Y* direction for all four displacement-orbits are shown in Figs. 6 through 9. The model exhibits good matching behavior for all of the displacement-based motions. Slight offsets are observed in analytical data for the square and figure-eight orbits. This is due to restrainer contact during the orbits. In general, using smaller displacement increments will in decrease this effect.

Figure 4. Rigid block experimental set-up at the UC Berkeley PEER Earthquake Simulator Laboratory.

Table 1. Geometry and friction of the TFP bearings used in the experimental characterization.

	Inner slider	Outer slider bottom	Outer slider top
Radius (in)	3.0	39.0	39.0
Height (in)	0.5	1.0	1.0
Outer diameter (in)	2.5	10.2	10.2
Inner diameter (in)	1.5	3.0	3.0
Friction coefficient	0.036	0.118	0.137

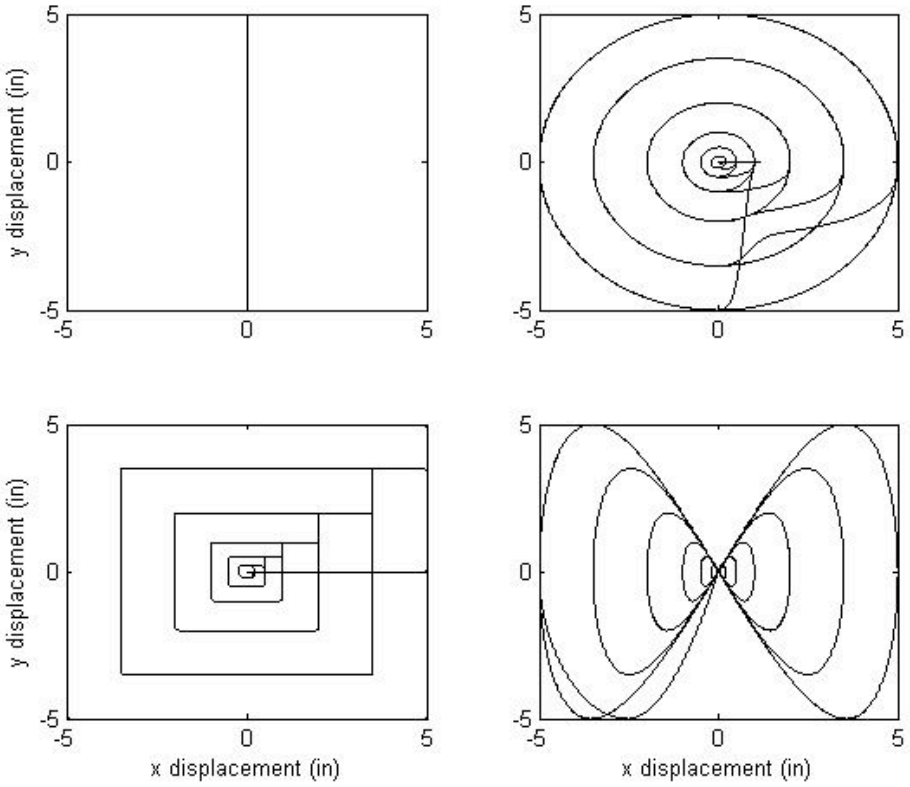

Figure 5. Displacement-controlled orbits used for bearing characterization including: sine waves, circles, squares and figure eights.

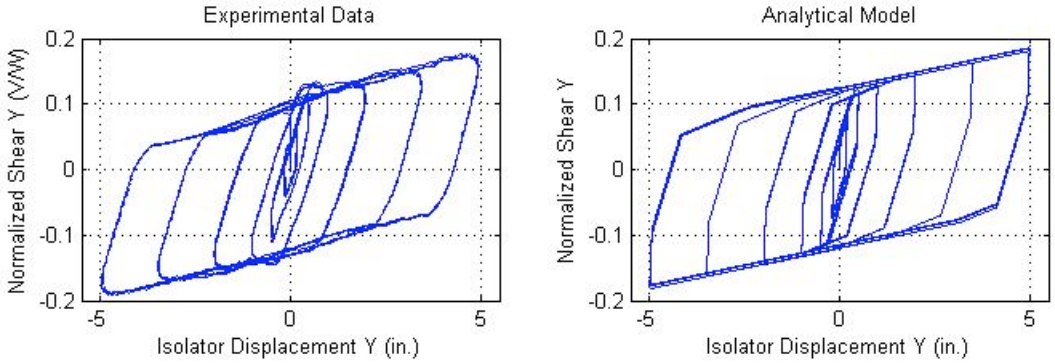

Figure 6. Experimental and analytical hystereses for the sine wave displacement orbit.

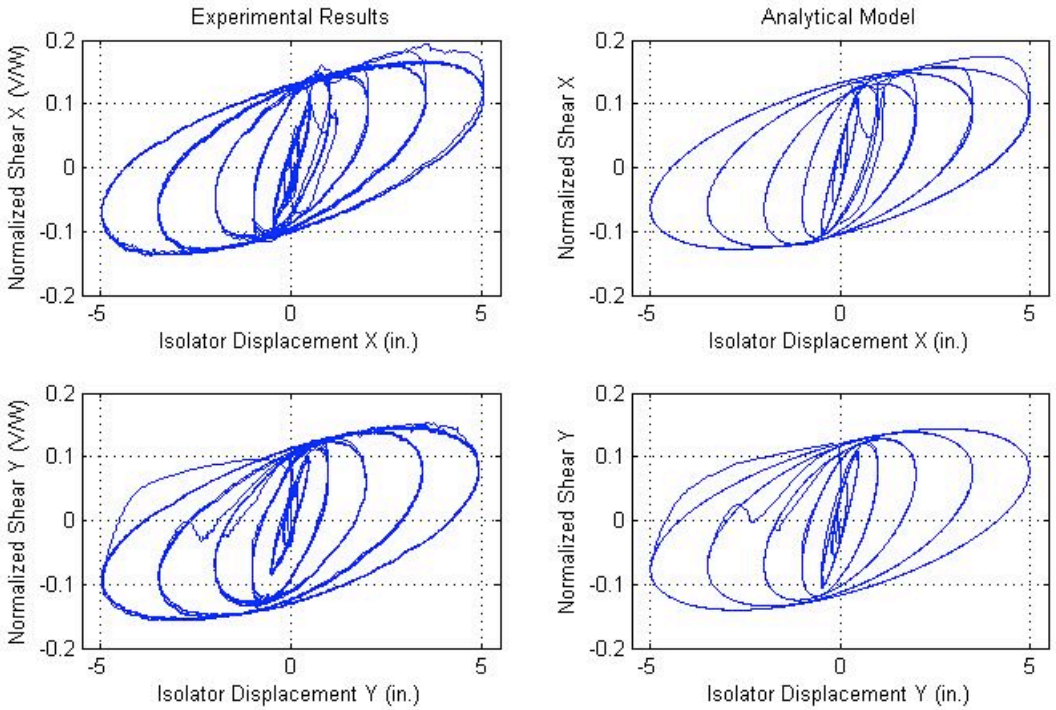

Figure 7. Experimental and analytical hystereses for the circular displacement orbit.

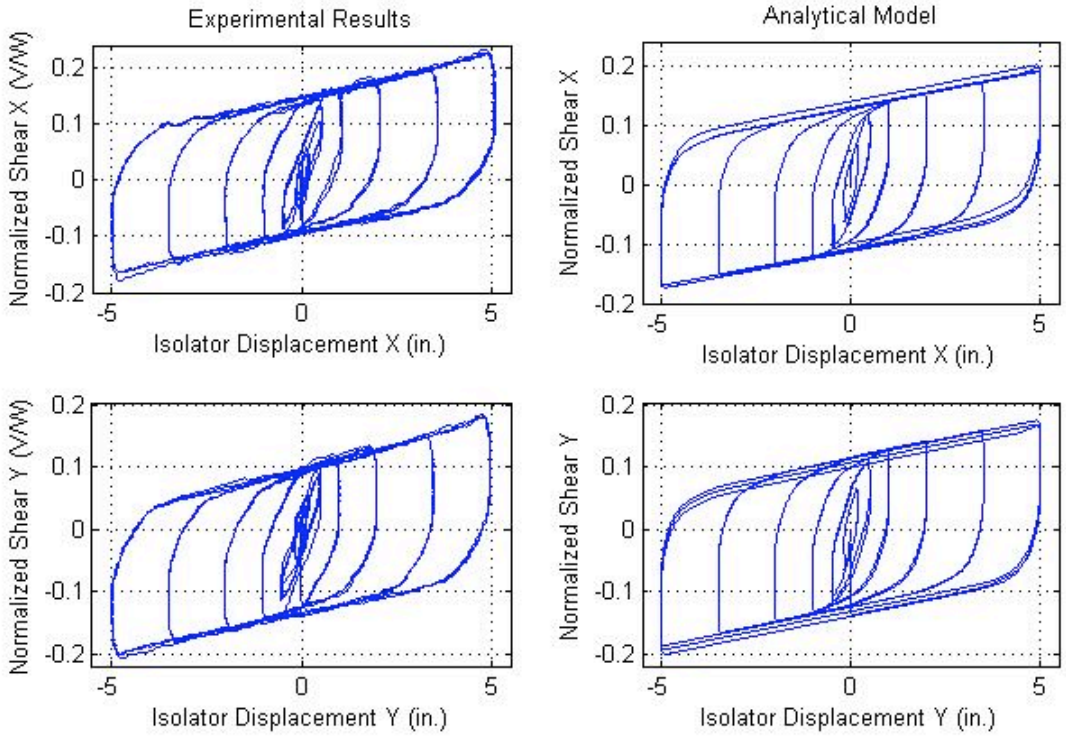

Figure 8. Experimental and analytical hystereses for the square displacement orbit.

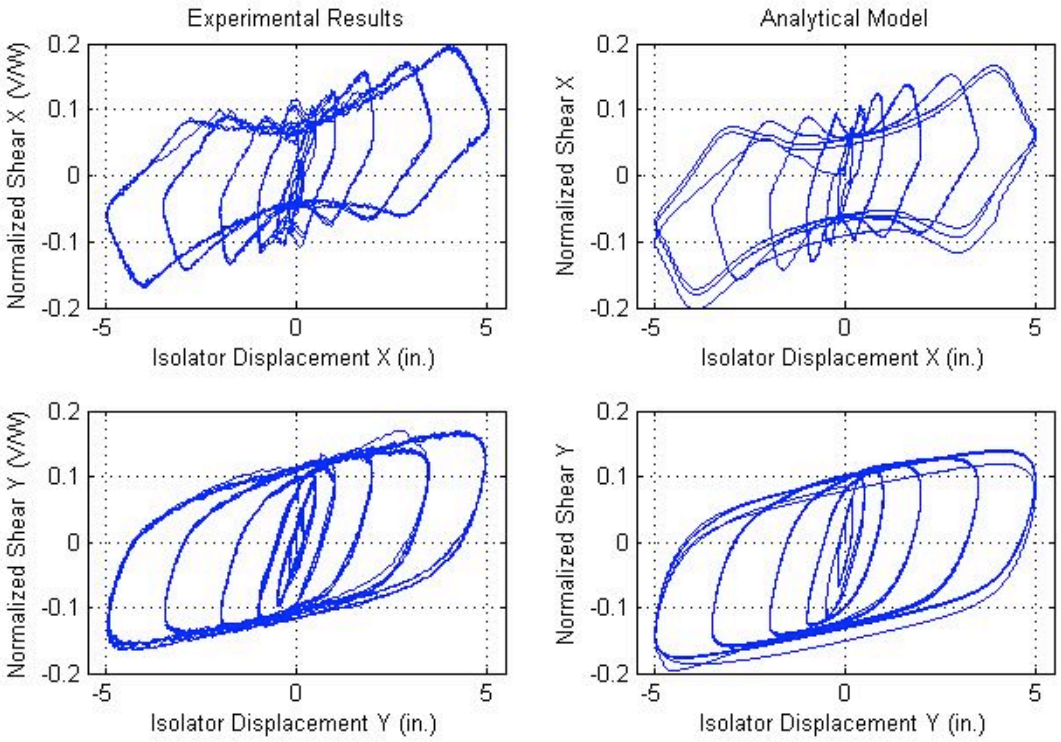

Figure 9. Experimental and analytical hystereses for the figure eight displacement orbit.

Future Considerations

Velocity, pressure and temperature all affect the friction coefficients of the four sliding layers. Changes in friction coefficients alter the force-displacement relationship of the TFP bearing. If the friction coefficients decrease, the displacement in the isolation layer of the building increases. If the friction coefficients increase, the superstructure will have higher lateral loads and damping. Thus, these effects are important to understand in order to estimate realistic building performance under earthquake loads. Effects on friction coefficient due to effects of velocity will be added to the model. A model for both this effect has been previously developed (Constantinou et al. 1990). Friction on each surface must be modeled independently as they vary in friction characteristics, and velocity.

Another aspect of TFP behavior to be investigated is the rotation about the vertical axis of the sliders as they move along restrainer surfaces. This motion increases the energy dissipated by the bearing. However, it remains to be seen if this has a significant effect on predicted behavior.

Conclusions

A 3D non-rotational model has been developed that accurately describes the behavior of TFP bearings. The model incorporates coupled plasticity and circular yield and restrainer surfaces. Additionally the effective pendulum length of the bearing is computed at each displacement. The model can accurately track the local displacements on each sliding surface. At

each displacement increment both the local and global forces and tangent stiffness matrices are calculated, making the model suitable for most structural modeling applications.

Acknowledgments

This paper is based upon work supported by the National Science Foundation under Grant No. CMMI-0724208. Any opinions, findings, and conclusions expressed here are those of the authors and do not necessarily reflect the views of the National Science Foundation. Thanks to Earthquake Protection Systems in Vallejo, California for providing the TFP bearings used in the experimental characterization and funding the tests.

References

Constantinou, M.C., Mokha, A., and Reinhorn, A.M. 1990. Teflon bearings in base isolation. II: Modeling, *Journal of Structural Engineering*, ASCE, 116 (2), 455-474.

Fenz, D.M. and M.C. Constantinou, 2008(a). Spherical sliding isolation bearings with adaptive behavior: Theory, *Earthquake Engineering and Structural Dynamics* 37 (2), 163-183.

Fenz, D.M, Constantinou, M. C, 2008(b) Development, implementation, and verification of dynamic analysis models for multi-spherical sliding bearings, *Report No. MCEER 08-0018.* Multidisciplinary Center for Earthquake Engineering Research, State University of New York at Buffalo.

Morgan, T.A. 2007. The Use of Innovative Base Isolation Systems to Achieve Complex Seismic Performance Objectives, *Doctoral Dissertation*, University of California Berkeley.

Morgan, T.A. and S.A. Mahin, 2008. The optimization of multi-stage friction pendulum isolators for loss mitigation considering a range of seismic hazard, *Proc.,* 14th World Conference on Earthquake Engineering, Beijing, China.

Mosqueda, G., Whittaker A. S., Fenves, G. L. and Mahin, S. A. 2004. Experimental and analytical studies of the friction pendulum system for the seismic protection of simple bridges, *Report No. EERC 2004-01,* Earthquake Engineering Research Center, Berkeley, CA.

Scheller, J. and Constantinou, M.C. 1999. Response history analysis of structures with seismic isolation and energy dissipation systems: Verification examples for program SAP2000, *Report No. MCEER 99-0002.* Multidisciplinary Center for Earthquake Engineering Research, State University of New York at Buffalo.

Simo, J. and Hughes T. 2000. *Computational Inelasticity (Interdisciplinary Applied Mathematics)*, Springer, New York.